© Österreichische
Geologische Gesellschaft/Austria; download unter www.geol-ges.at/ und www.biologiezentrum.at

Austrian Journal of Earth Sciences | Volume 106/2 | 63 - 74 | Vienna | 2013

Pre-Alpine fold interference patterns in the northeastern Oetztal-Stubai-Complex (Tyrol, Austria)

Mathias EGGLSEDER[1)2)*)], Bernhard FÜGENSCHUH[1)]

[1)] Department of Geology and Paleontology, University of Innsbruck, Austria;

[2)] School of Geosciences, Monash University, Melbourne, Australia;

[*)] Corresponding author, mathias.egglseder@monash.edu

KEYWORDS

fold interference pattern
Oetztal-Stubai-Complex
pre-Alpine deformation
superposed folding
Brenner Mesozoic
Variscan orogeny

Abstract

Structural geological investigations near the base of the Brenner Mesozoic (BM) of the northeastern Oetztal-Stubai-Complex (OSC) showed evidence for polyphase Variscan folding of the OSC in comparison to Alpine structures of its Permomesozoic cover (BM). Local remapping in the Kalkkoegel area (northern BM) revealed an unknown first isoclinal folding event (D_1) with S- and NE-orientated folds that formed a penetrative schistosity subparallel to the bedding ($S_{0/1}$). Large-scale open folding with ESE- and WNW-trending fold hinges overprinted this $S_{0/1}$-foliation with the development of a S_2-foliation and resulted in regional-scale intermediate Type 2/Type 3 fold interference patterns. Reverse modelling of these "elongated mushroom-shaped" geometries led to a newly established simple pseudo-stratigraphy, with meta-igneous rocks intruding into paragneisses overlain by mica schists. After Permomesozoic strata (BM) were deposited discordantly on top of the OSC, both were overprinted by ductile and brittle deformation during the Cretaceous (D_3 & D_4) and Cenozoic (D_5 & D_6) Alpine orogenies. Brittle deformation is still ongoing, as displayed by seismic activity related to the northward movement of the Southalpine indenter.

Strukturgeologische Untersuchungen im Nordosten des Ötztal-Stubai-Komplexes (OSC) an der Basis des Brennermesozoikums (BM) lieferten neue Einblicke in die duktile polyphase variszische Deformationsgeschichte im OSC durch Vergleich mit alpidischen Strukturen in den überlagernden permomesozoischen Decksedimenten (BM). Durch lokale Kartierungen im Bereich der Kalkkögel (nördliches BM) konnte eine bisher unbekannte erste isoklinale Verfaltung (D_1) mit S- und NE-orientierten Falten festgestellt werden, die zur Bildung einer penetrativen Schieferung subparallel zur sedimentären Schichtung ($S_{0/1}$) führte. Eine zweite großmassstäbliche offene ESE-orientierte Verfaltung überprägte diese $S_{0/1}$-Schieferung mit der Bildung einer S_2-Schieferung und führte zur Bildung von intermediären Typ 2/Typ 3 Faltenüberprägungen. Reverse modelling ermöglichte die Interpretation dieser „gestreckten pilzförmigen" Muster und die Einführung einer Pseudo-Stratigraphie mit metamorphen Plutoniten/Vulkaniten an der Basis, die in Paragneisse intrudiert sind und von Glimmerschiefern überlagert werden. Nach der diskordanten Sedimentation permomesozoischer Einheiten (BM) auf dem OSC, wurden beide Einheiten während beiden alpidischen Orogenesen in der Kreide (D_3 & D_4) und im Känozoikum (D_5 & D_6) duktil und spröd deformiert. Die anhaltende spröde Deformation durch die nordwärts-gerichtete Bewegung des Südalpinen Indenters ist anhand seismischer Aktivitäten immer noch feststellbar.

1. Introduction

The Oetzal Stubai Complex (OSC) of Tyrol, Austria, has been intensively investigated with a petrographic, petrological and geochronological focus (e.g. Miller, 1970; Hoernes and Hoffer, 1973; Veltman, 1986; Söllner and Hansen, 1987; Miller and Thöni, 1995; Klötzli-Chowanetz et al., 1997; Thöni, 1999, Tropper and Recheis, 2003). While petrological highlights such as migmatites, eclogites and mica schists attracted numerous scientists, the rather monotonous but widespread paragneisses of the OSC were hardly ever studied. Since the classic works on the OSC by Tollmann (1963, 1977), Schmidegg (1964), Purtscheller (1971, 1978), Thöni (1980, 1981) and Hoinkes et al. (1982) general structural investigations addressing the entire OSC are lacking. Structural and tectonic aspects of the OSC have mostly been carried out within relatively local geological contexts (e.g. Schmidegg, 1964; Förster, 1967; Förster and Schmitz-Wiechowski, 1970; van Gool et al., 1987; Fügenschuh et al., 2000; Sölva et al., 2005). In this investigation, we attempt to decipher the polyphase structural evolution of the northeastern part of the OSC, with a special focus on pre-Alpine folding events, and we compare our findings to those of Alpine deformation events recorded in its Permomesozoic cover, the Brenner Mesozoic (BM).

This study is based on regional mapping at the scale of 1:10,000 in the Kalkkoegel area in the northeasternmost portion of the OSC and BM. The post-Variscan age of the cover units enabled us to distinguish pre-Alpine structures in the OSC from Alpine structures in the BM. With the integration of a simplified version of the geological map sheet "Oetzthal" of Hammer (1929), local structural observations were interpreted in the context of a regional-scale fold interference pattern.

2. Geological Setting

The OSC is a basement complex located in the central Alps (Fig. 1) and is tectonically attributed to the Oetztal-Bundschuh-Complex, with the OSC west and the Bundschuh-Complex east of the Tauern window (Schmid et al., 2004). Although this

© Österreichische
Geologische Gesellschaft/Austria; download unter www.geol-ges.at/ und www.biologiezentrum.at

attribution is still controversial (Neubauer et al., 2007), we assume that within the context of Alpine nappe stacking both complexes have similar positions. Following the palinspastic restoration of Frisch et al. (1998), both these complexes were connected prior to the eastern lateral escape of the Eastern Alps towards the retreating subduction zone in the Carpathians (Royden et al., 1982) in response to the northward movement of the Southalpine indenter and the Miocene exhumation of the Tauern window.

In the northernmost part of the BM, (i.e. the Kalkkoegel area) the stratigraphy encompasses a sequence of transgressive sediments deposited onto a paleo-weathering horizon of the uppermost OSC (Krois et al., 1990). The deposition was initiated by Permo-Triassic clastics of the Alpine Verrucano, followed by dolomites and marls of the Virgloria Formation, Reifling Formation and Partnach Formation that interfinger with dolomites of the Wetterstein Formation. These successions are sealed by the Raibl shales, and the Norian Hauptdolomite completes the sequence with dolostone units (Rockenschaub et al., 2003; Brandner et al., 2003; Brandner and Reiter, 2004). The hanging wall units of the W-dipping Brenner fault zone are tilted towards the east and thus preserved the parautochthonous BM (Köhler, 1978; Krois, 1989) from erosion in the vicinity of the fault zone in the eastern part of the OSC.

The OSC consists of metamorphic rocks with various protoliths: orthogneisses of plutonic origin, amphibolites of volcanic and plutonic origin, and metapelites and metapsammites of sedimentary origin. Paragneisses are considered to be the oldest rocks in the OSC with a mean crustal residence age of ca. 1.5 Ga (Schweigl, 1995) to 1.6 Ga (Thöni, 1999). Meta-igneous rocks, which intruded the meta-sediments, have protolith ages ranging from 520-530 Ma for mafic intrusions (Schweigl, 1995) and 485 ± 3 Ma for intrusions with granitic compositions (Bernhard et al., 1996). Paleogeographically, the OSC formed part of the Apulian margin and is tectonically attributed to the Upper Austroalpine nappe complex (e.g. Schuster and Frank, 1999; Schmid et al., 2004), which formed through WNW-directed thrusting during the Cretaceous (Eoalpine) orogeny (Frank et al., 1987; Froitzheim et al., 1994).

The OSC is entirely fault bounded, with the different faults having different kinematics and ages (Fig. 1). They consist of the Inntal fault to the north (Ortner et al., 2006), the Brenner fault zone to the east (Fügenschuh, 1995), the Schneeberg fault zone and Vinschgau shear zone to the south (Flöss, 2009; Speckbacher, 2009; Sölva et al., 2005), the Schlinig fault to the west (Schmid and Haas, 1989) and the Engadine line to the northwest (Schmid and Froitzheim, 1993).

3. Polymetamorphism

The OSC is well known for its polymetamorphic evolution (i.a. Hoinkes et al., 1982; Thöni, 1999) with the youngest metamorphic event (i.e. Eoalpine orogeny) being of Cretaceous age (Frank et al., 1987), which reaches lower greenschist facies in the NW corner of the OSC and increases towards the SE to upper amphibolite grade conditions, with eclogite facies conditions documented in the underlying Texel complex (Thöni, 1980, 1981; Hoinkes et al., 1991; Konzett and Hoinkes, 1996). This regional variation in metamorphism is reflected in an increase from 445 °C in the north to 530 °C in the south within the BM (Hoernes and Friedrichsen, 1978; Tessadri, 1981; Dietrich, 1983). Eoalpine metamorphism within the Kalkkoegel area reached temperatures of about 450 °C (Hoernes and Friedrichsen, 1978) whereas temperatures during the pre-Alpine metamorphic event were substantially higher (ca. 600 °C: Hoernes and Friedrichsen, 1978).

Purtscheller (1978) documented a Variscan metamorphic zonation in the OSC based on the distribution of aluminosilicates (Fig.1). However, this zonation is questioned by Hoinkes and Thöni (1993) and Tropper and Recheis (2003), who propose that although the zonation is consistent with the metamorphic gradient between the Variscan and Alpine orogenies, the aluminosilicates do not necessarily represent a single metamorphic event. Schuster et al. (2004) estimated the age of the Variscan thermal peak at 340 Ma and Variscan cooling ages at ca. 310 Ma (Miller and Thöni, 1995; Neubauer et al., 1999; Thöni, 1999) with maximum Variscan temperatures of 670 °C in the northern area of the OSC (Hoinkes et al., 1982).

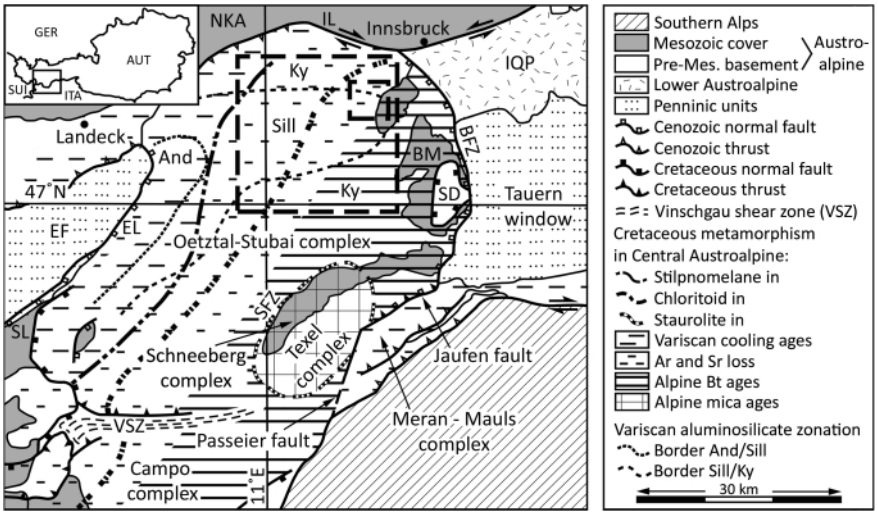

Figure 1: Tectonic overview of the Oetztal-Stubai-Complex showing the distribution of Cretaceous metamorphism (redrawn after Fügenschuh et al., 2000), small dashed rectangle: study area, large dashed rectangle: extent of geological map of Hammer (1929). BFZ = Brenner fault zone, BM = Brenner Mesozoic, EF = Engadine window, EL = Engadine line, IL = Inntal line, IQP = Innsbruck Quartzphyllite, NKA = Northern Calcareous Alps, SD = Steinach nappe, SL = Schlinig line, SFZ = Schneeberg fault zone, VSZ = Vinschgau shear zone. Variscan aluminosilicate zonation after Purtscheller (1969): And = Andalusite zone, Ky = Kyanite zone, Sill = Sillimanite zone.

© Österreichische
Geologische Gesellschaft/Austria; download unter www.geol-ges.at/ und www.biologiezentrum.at

For the eclogites in the central Oetztal, PT conditions of 27 kbar and 730 °C, together with an age of 370-340 Ma, were determined by geothermobarometry and Sm-Nd mineral isochrons (Miller and Thöni, 1995). The oldest metamorphic event within the OSC is represented by Ordovician/Silurian migmatites of the Winnebach area, for which Klötzli-Chowanetz et al. (1997) and Thöny et al. (2008) determined ages ranging between 490 ± 9 Ma (U/Pb zircon age) and 441 ± 18 Ma (U-Th-Pb electron microprobe monazite age).

The metamorphic evolution of the OSC is well-documented, whereas structural investigations are rather scarce (e.g. van Gool et al., 1987; Sölva et al., 2005). Although a clear attribution of structural elements to the different tectonometamorphic events has not been proposed yet, it is our understanding that differences in metamorphic grades were essential to classify observed structures as Alpine or Variscan deformational events.

4. Deformation stages

The OSC is dominated by large-scale E-W-striking open folds. However, the exact location of their major axial traces were not clearly mapped at this stage, partly because of numerous non-cylindrical parasitic folds and a discontinuous appearance of lithologies due to boudinage. Despite these difficulties structural observations and regional map patterns can be interpreted in the following proposed deformation sequence.

4.1 Deformation stage D_1

D_1 is defined by a penetrative schistosity (S_1) formed by biotite and muscovite in amphibolite facies conditions and by the occurrence of garnet, staurolite and kyanite. D_1 is related to large amplitude (up to 100m scale) isoclinal folding and the main foliation can be addressed as a composite $S_{0/1}$ planar feature because S_1 is subparallel to the observed bedding. Main observations related to D_1 are (1) isoclinal and often intrafolial folds, (2) slightly S- or NE-plunging fold hinges (F_1), (3) mainly NE- and S-trending mineral stretching lineations (L_1) (sub-) parallel to the fold hinges and (4) slightly ESE- and WNW-dipping $S_{0/1}$-axial planes (Fig. 2, left).

Due to the parallelism of F_1 and L_1, D_1 folds could be interpreted either as sheath folds (Alsop and Carreras, 2007) or as isoclinal folds originally formed parallel to the stretching direction during intense shearing (Grujić and Mancktelow, 1995). The latter interpretation is favoured because the NE-SW trending stretching lineations point to shearing along this direction, but no unequivocal shear sense could be determined with respect to the D_1 stretching lineation. Further investigations are necessary to verify the geodynamic meaning of D_1.

4.2 Deformation stage D2

This deformation phase forms the dominant structures within the OSC and refolds the $S_{0/1}$ foliation (Fig. 3a, b). It is characterized by (1) sub-horizontal ESE- and WNW-plunging non-cylindrical parasitic folds (F_2) of different orders associated with open folds with kilometer-scale amplitudes, (2) sub-horizontal ESE- and WNW-orientated mineral stretching lineations L_2 and (3) steeply N- and S-dipping S_2 foliations with a similar mineral assemblage as S_1 (Fig. 2, left).

This superimposed folding leads to a strong parallelism of F_1 and F_2 that results in subparallel $S_{0/1}$- and S_2-foliations. These foliations can only be clearly identified in D_2 hinge zones where F_1 and F_2 remain more or less in their original orientation. D_1 and D_2 are responsible for the penetrative foliation generally observed throughout the whole OSC. Due to their great overlap in terms of metamorphic grade and geometry of structural elements, D_1 and D_2 are proposed to represent ongoing deformation during one protracted Variscan

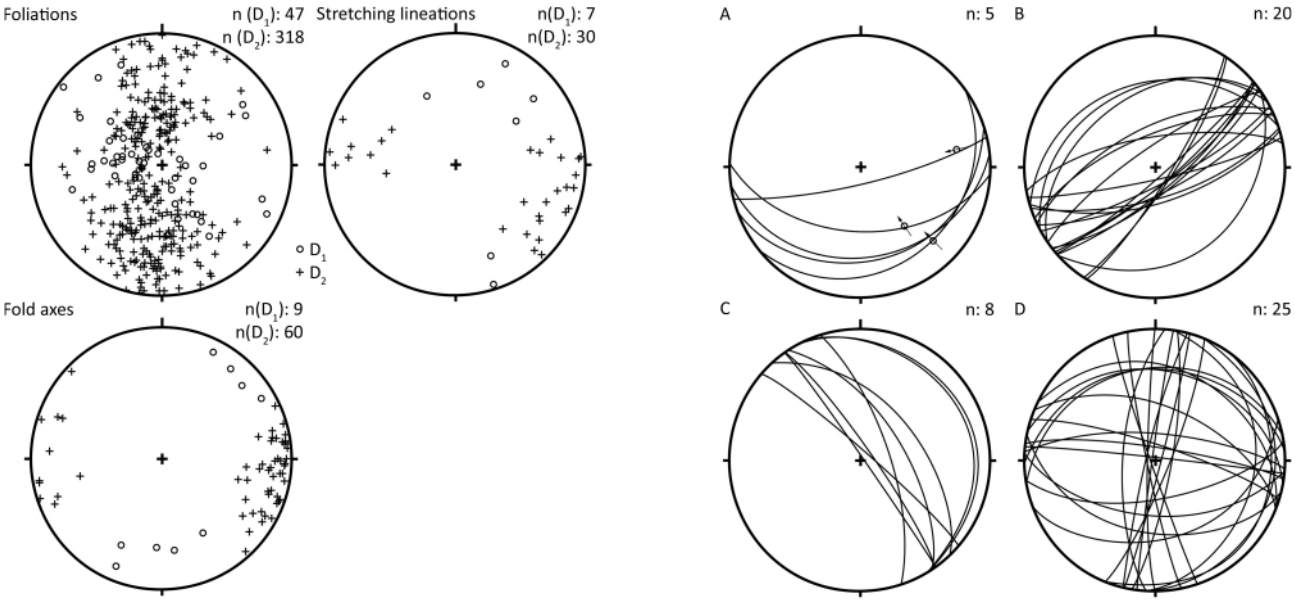

Figure 2: Structural data of the investigation area: (left) comparison of D_1 and D_2 foliations, stretching lineations and fold hinges; (right) A: NNW- and W-orientated D_5 thrusts, B: brittle faults related to the Stubaital fault, C: brittle faults related to the Halsl fault, D: brittle faults in the hanging wall of the Brenner fault.

© Österreichische
Geologische Gesellschaft/Austria; download unter www.geol-ges.at/ und www.biologiezentrum.at

tectonometamorphic event. D_1 and D_2 are clearly pre-Alpine since their axial traces and foliations are not observed within the BM and are discordant to the stratigraphic base of the BM (Krois et al., 1990).

4.3 Deformation stage D_3

This deformation stage is manifested by rarely observed W to NW-directed thrust faults and is interpreted to be related to Cretaceous thrusting (i.e., Trupchun phase, Froitzheim et al., 1994). D_3-structures are only hardly observable due to later overprinting and, according to Purtscheller (1978) and Fügenschuh et al. (2000), are restricted to the top of the OSC.

4.4 Deformation stage D_4

Subhorizontal to slightly SE-dipping foliations are developed along shear zones with top-to-the-SE directed shearing. Related folds have meter-scale amplitudes and show similar orientations as kilometer-scale D_2 folds in the OSC. However, due to differences in scale and qualitative determination of forming temperatures from thin section inspections (e.g. green biotite in BM: greenschist facies; brown biotite in OSC: amphibolite facies) these structures are instead attributed to a late Cretaceous extension event (Ducan-Ela phase, Froitzheim et al., 1994), which affected the uppermost part of the OSC close to the BM contact, whereas most of the deformation was taken up by the Mesozoic cover sequences. Moreover, planar SE-orientated normal faults led to the SE-dipping foliation subparallel to the bedding in the BM (Rockenschaub et al., 2003) and equivalent SE-orientated crenulation lineations or fault propagation folds in the OSC (Fig. 3c). The contact between the OSC and its cover (BM) is termed parautochthonous (Köhler, 1978; Krois, 1989) because only minor amounts of shearing occurred at this boundary.

4.5 Deformation stage D_5

Small-scale NNW- to SSE-vergent brittle thrusts were observable throughout the field area (Fig. 2A) but due to their limited extent do not show up on map scale. Mica-rich units of the OSC show a weak crenulation (Fig. 3d) with ENE-trending fold hinges, in accordance with observations made by Langheinrich (1965). Both their orientations (folds and thrusts) and kinematics (thrusts) are consistent with Cenozoic thrusting of Austroalpine units upon Penninic units (Rockenschaub et al., 2003), i.e. the Blaisun phase of Froitzheim et al. (1994).

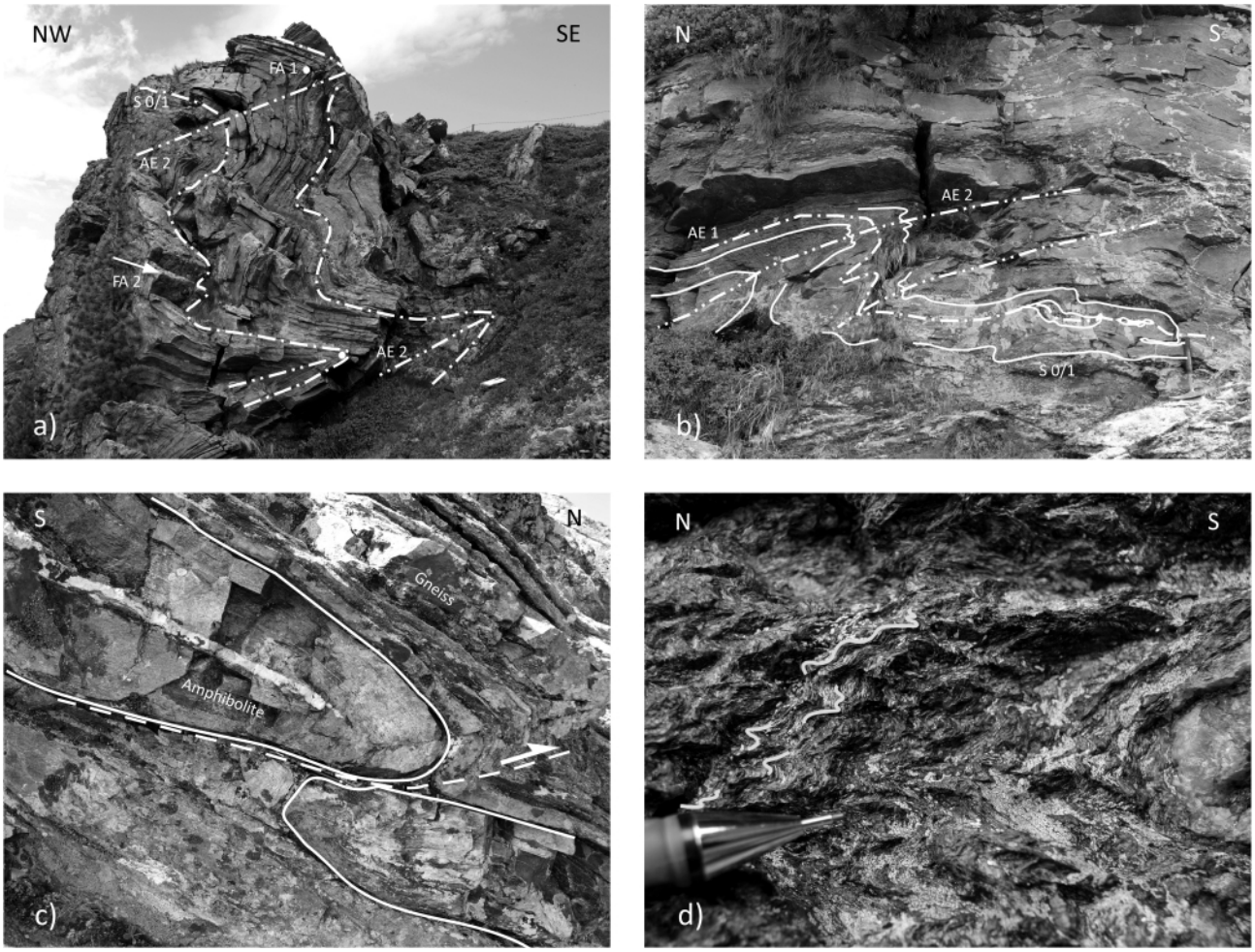

Figure 3: Outcrop scale structures: (a) D_2 hinge zone with refolded $S_{0/1}$, (b) south-vergent D_2 parasitic fold refolding isoclinal D_1 fold, (c) thrusting of originally (D_1) boudinaged amphibolite in a D_2 fault propagation fold, (d) D_5 crenulation in mica schist.

© Österreichische
Geologische Gesellschaft/Austria; download unter www.geol-ges.at/ und www.biologiezentrum.at

Independent evidence for this interpretation is pending.

4.6 Deformation stage D_6

Both from overprinting criteria and geometrical considerations, the youngest phase of deformation is related to deformation of the OSC and BM in the hangingwall of the Brenner fault zone (Fügenschuh et al., 1997). This fully brittle stage is evidenced by NE- (e.g. Stubaital fault, Fig. 2B) and NW-trending (e.g. Halsl fault, Fig. 2C) strike-slip faults together with N-S-trending normal faults (e.g. Seejoechl fault, Fig. 2D). Brittle deformation started essentially during the Neogene and has remained active until recent times (Reiter et al., 2005). The relative timing of activity along these faults, as proposed by Rockenschaub et al. (2003), cannot be verified because of a lack of exposure of cross-cutting relationships.

5. Model

The OSC is a polyphase folded complex, a fact already known and described by several authors (e.g., Schmidegg, 1956; Tollmann, 1963; 1977; Purtscheller, 1971; 1978; van Gool et al., 1987). A qualitative description of D_2 folds (in our notation) dates already back to Hammer (1929), but was not elaborated in a more genetic context. Only van Gool et al. (1987) investigated structures in the SW of the OSC, which show some similarities to the observed structures in the NE. The main problem with correlating the findings of van Gool et al. (1987) from the southernmost OSC with the structures in the north is the substantially stronger Cretaceous overprint in the south, where Eoalpine metamorphism reached amphibolite facies conditions. On the contrary, structures of the southernmost OSC are more likely related to Cretaceous tectonics than by Variscan deformation (Pomella et al., 2010).

Firstly, the observed two-phase folding is displayed by the two different sets of fold hinges and stretching lineations and the mutual fold interference in outcrops. Outcrop-scale fold interference patterns are largely of Type 3 (Ramsay, 1967), whereas the incorporation of the geological map of Hammer (1929) provides a more regional perspective showing a mixed

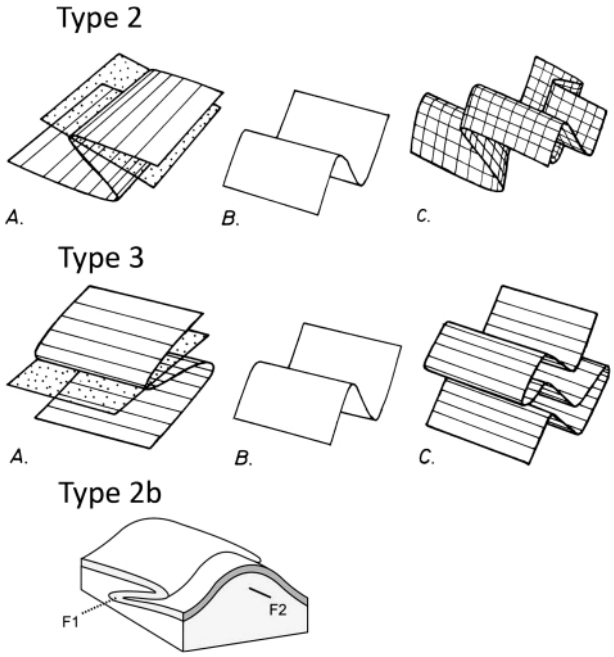

Figure 4: Type 2 and Type 3 fold geometries (Ramsay and Huber, 1987): (A) initial folding, (B) superposed folding, (C) resulting fold geometry and Type 2b fold geometry (Simón, 2004): (F1) initial fold axis of isoclinal folds, (F2) overprinting fold axis of open folds.

Type 2/Type 3 fold interference pattern. The difference between Type 2 and Type 3 fold interferences is the orientation of initial folding and can be seen in Fig. 4. Type 2 superimposed folding leads to folding of both initial fold hinges and axial planes in contrast to Type 3 folding, which results in subparallel fold hinges without folding of the pre-existing fold hinges. Pure Type 2 fold interferences show mushroom-shaped outcrop patterns (Fig. 5, 90° between fold hinges and axial planes) and with decreasing angle between the two fold hinges the mushroom pattern becomes elongated (Fig. 5, 45° and 20°). The evidences described above indicate that the angle is likely 20-30° between D_1 and D_2 fold hinges, whereas the initial orientation of D_1 and D_2 axial planes is estimated as perpendicular, but according to Odonne and Vialon (1987)

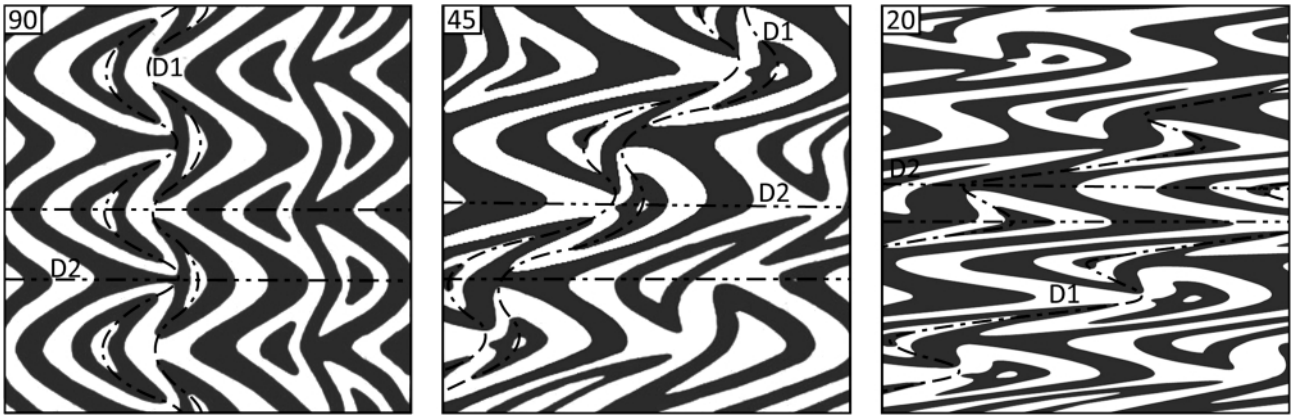

Figure 5: Fold interference pattern after Ramsay and Huber (1987): (90) typical Type 2 interference pattern with perpendicular fold hinges and axial planes, (45) intermediate Type 2/Type 3 interference pattern with an angle of 45°, (20) intermediate Type 2/Type 3 interference pattern with an angle of 20° illustrating differently stretched mushroom-shaped pattern.

© Österreichische
Geologische Gesellschaft/Austria; download unter www.geol-ges.at/ und www.biologiezentrum.at

Figure 6: Digitized geological map sheet “Oetzthal” of Hammer (1929) (1:175,000). For legend see Fig. 8.

© Österreichische
Geologische Gesellschaft/Austria; download unter www.geol-ges.at/ und www.biologiezentrum.at

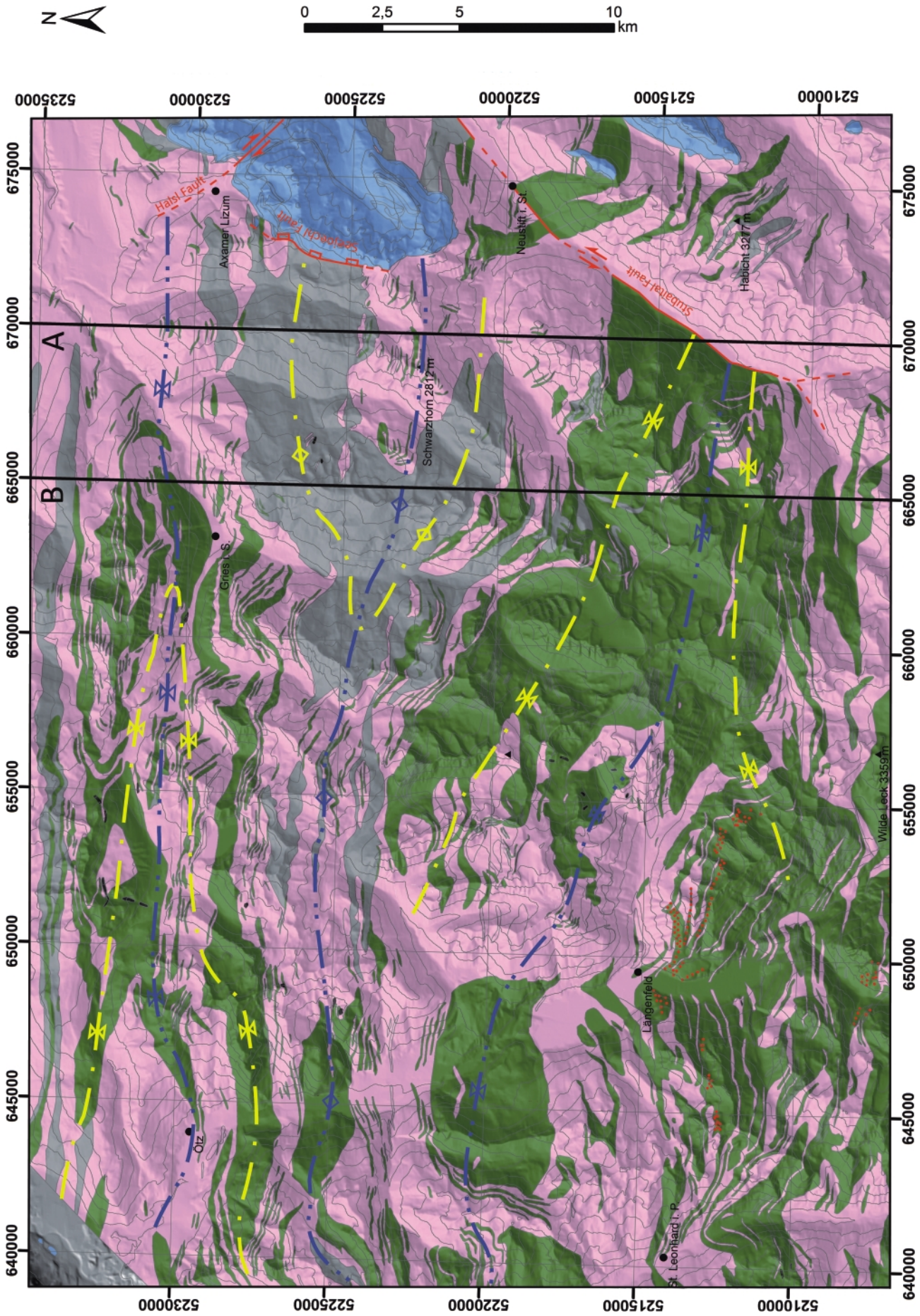

Figure 7: Simplified geological map “Oetzthal” of Hammer (1929) (1:175,000). For simplification of lithologies see Fig. 8.

© Österreichische
Geologische Gesellschaft/Austria; download unter www.geol-ges.at/ und www.biologiezentrum.at

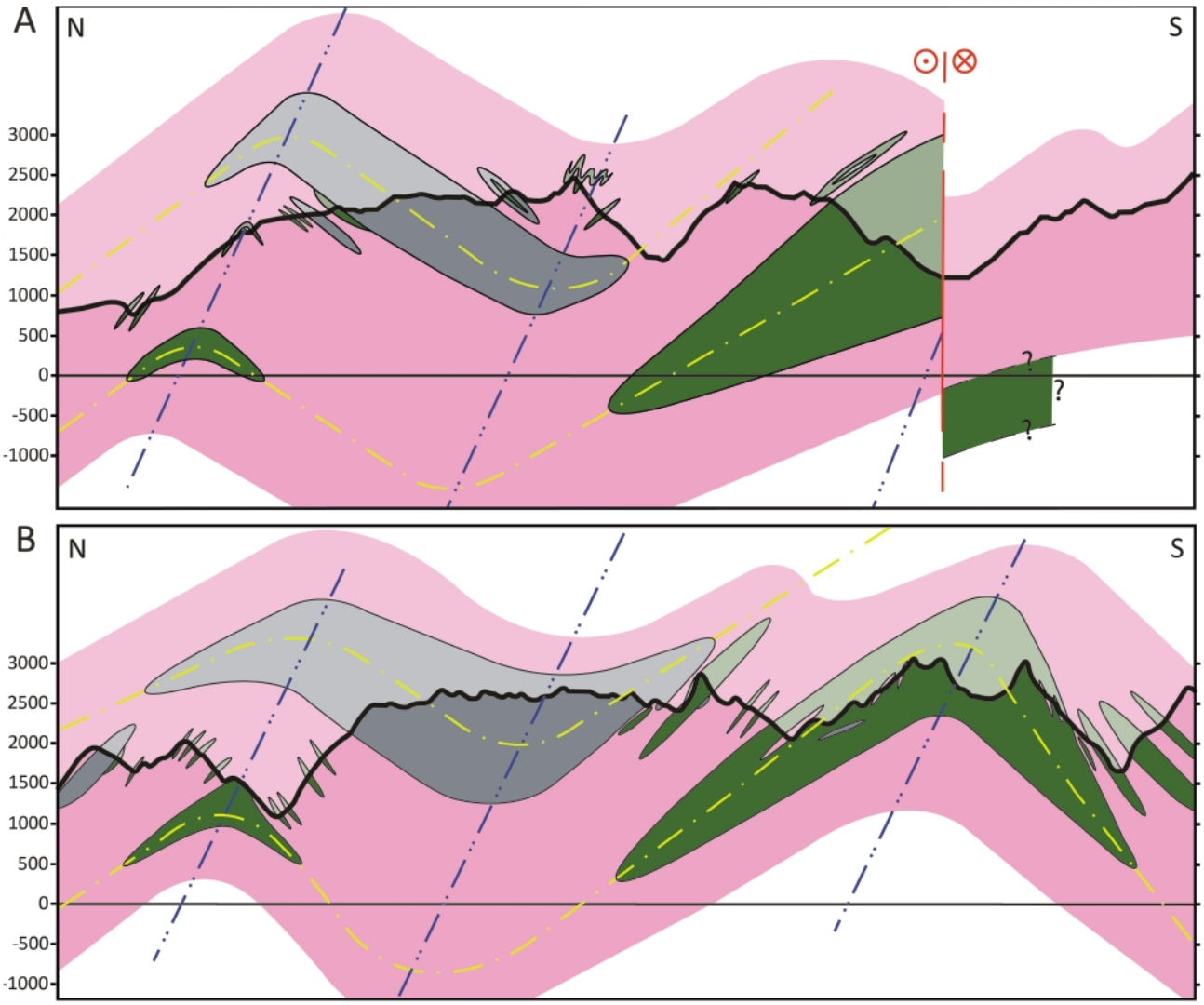

Legend

Quaternary sediments

- Alluvial fan
- *qz* Interglacial terrace deposits
- *qm2* Moraines (Inn valley glacier)
- *qm3* Moraines of tributary valley glaciers (stages of retreat)
- *rbt* Rockslides of triassic rocks
- *rb* Rockslides of gneisses
- *r* Young debris fans
- Glaciers
- Young moraines and alluvial deposits
- Marsh

Brenner Mesozoic

- *td* Haupt dolomite
- *tl* Raiblian schists
- *twd* Wetterstein dolomite
- *tm* Basal rocks of the Kalkkoegel
- *p* Permotriassic quartzite and quartz conglomerate
- *pe* Mineralized quartz conglomerate

Oetztal Stubai Complex

- *Di* Diabasic dike rocks
- *Dk* Diorite, Kersantite diabase

Mica schists

- *pk* Mica schists, garnet- and staurolite-bearing

Paragneisses

- *ch* Chlorite schists, greenschist
- *g_* Scaly biotite gneiss
- *gb1* Bt-Pl-gneiss (schist gneiss) & gneiss mica schists
- *gb1x* Crd-bearing Bt-granite & migmatite
- *gb1~* Mylonitic biotite plagioclase gneiss
- *gu* Quartzite

Amphibolite / Orthogneisses

- *G'* Biotite granite gneiss
- *G'~* Biotite granite gneiss mylonitic
- *G'o* Biotite Augengneiss
- *G'o~* Biotite Augengneiss mylonitic
- *Ga* Dark- & white mica-bearing Augen- & Flasergneiss
- *Gb* Porphyroblastic Bt-granite- & injection gneiss
- *Gc* Crd-bearing Bt-granite & migmatite
- *Gm* Muscovite granite gneiss, aplites and pegmatites
- *Gm~* Muscovite granite gneiss mylonitic
- *Go* Granodiorite gneiss
- *Gp* Crd-bearing porphyry granite & granite gneiss
- *gb* Fine-grained biotite schists
- *gbx* Crd-bearing biotite schists and migmatites
- *gbxx* Crd-bearing biotite schists and migmatites
- *gh* Hbl-Bt-gneiss & Bt-orthogneiss of amphibolitic zones
- *gq* Quartzites intercalated with biotite schists
- *hf* Amphibolite and hornblende schists

Line features

- Eclogitic zone
- Feldspar-knot formation
- Faults
- Faults (assumed)
- Strike-slip fault
- Normal fault
- D1-Axial trace
- D2-Axial trace

Mineral abbreviations

Bt	Biotite	Hbl	Hornblende
Crd	Cordierite	Pl	Plagioclase

Figure 8: top: Cross sections A and B, axial traces indicated in Fig. 7; bottom: Legend to Fig. 6 to Fig. 8, (right squares indicating original lithological classification of Hammer, 1929 and left squares summarized in parentheses indicating reduced lithologies of Fig. 7 and Fig. 8, top).

© Österreichische
Geologische Gesellschaft/Austria; download unter www.geol-ges.at/ und www.biologiezentrum.at

directions of fold axes in areas of superposed folding cannot be used to determine compression directions.

Ghosh (1974) and Skjernaa (1975) distinguished, on the basis of physical experiments, that overprinting folds are cylindrical if the first folding event is tight or isoclinal, but low-cylindrical when first folds are rather open. Ghosh et al. (1992) also determined that fourth mode superposed buckling (Type 2b; Simón, 2004; Fig. 4) in contrast to third mode (Type 2a; Simón, 2004) consists of isoclinal D_1 folds with folded hinges and axial planes because of refolding by D_2. Although the cylindricity of D_1 folds, local thickness variations and viscosity contrasts of lithologies were neglected, these theoretical assumptions are consistent with the pattern observed in the investigated part of the OSC.

Ghosh (1974) and Grujić (1993) investigated Type 1/Type 2 fold interferences and determined that "strong shear strains develop along the hinge zones of those early folds that are located at the limbs of the later folds. This will rotate any lineation, which was not parallel to the first fold hinge line into parallelism with it." Transferred to Type 2/Type 3 fold interferences this parallelization of the D_1 hinges and D_2 hinges results in the observed outcrop-scale Type 3 fold interference patterns in D_2 limb zones and intermediate Type 2/Type 3 fold interference pattern could only be observed in D_2 hinge zones.

Type 2 interference patterns become much more evident after redrawing and simplifying Hammer's map (Fig. 6) and combining of the originally depicted lithologies to essentially three lithological groups (Fig. 7): (1) Paragneisses, (2) micaschists and (3) magmatics (felsic and mafic). Although this simplification might ignore local lithological details and variations, we insist on the regional coherence. The combination of felsic and mafic magmatic rocks was mainly done due to their rather discontinuous pattern, a feature resulting from their relatively higher competency during deformation and, consequently, their appearance as boudins. Moreover it has to be stated that the distinction of D_1 antiforms from synforms could not be carried out unequivocally. We based our interpretation on a pseudo-stratigraphy only for working purposes, which is made up of (from bottom to top) (1) magmatic rocks, (2) paragneisses and (3) micaschists. Based on this stratigraphy micaschists are found in the cores of synforms while amphibolites and orthogneisses form the cores of antiforms (Fig. 8, top). The effect of lateral thickness variations can be observed due to the initial isoclinal D1 folding and can be assumed for the entire northeastern part of the OSC (Fig. 8, top).

6. Discussion

The geodynamic setting of the investigated area is difficult to determine due to the lack of detailed investigations on the relation between metamorphism, deformation and related geochronological data. For the eclogites and migmatites of the central OSC, excellent petrological and geochronological data are available, but no correlation with different stages of deformation has been worked out at this point.

While meta-igneous rocks are associated with paragneisses and could then be syn- or postdepositional to them, qualitatively micaschists are almost exclusively free of magmatic rocks and could represent a late to post-magmatic formation.

The OSC was substantially affected by the tectonometamorphic overprint related to the Variscan orogeny (Maggetti and Flisch, 1993; von Raumer and Neubauer, 1993), which led to a still preserved metamorphic zonation, especially in its northern part (cf. Fig. 1), as well as a dominant E-W striking composite penetrative foliation. The D_1 structures are either related to this Variscan cycle, or could date back to an even earlier Ordovician-Silurian tectonism, coeval to migmatites of the central OSC (Schweigl, 1995; Thöni, 1999). Here, we assume a Variscan age for both our folding stages, since structures related to D_1 fit well with the known Variscan metamorphic temperatures of 469 - 630 °C and 4.2 – 7.3 kbar for the northern part of the OSC (Tropper and Recheis, 2003). Furthermore, the orthogneisses in the OSC, which are dated as Cambrian to Silurian, are affected by D_1 and D_2 (Thöni, 1999). The first phase (D_1) formed isoclinal folds with sub-horizontal fold axial planes. The second phase (D_2) developed kilometer-scale relatively open folds with subvertical, recently inclined fold axial planes. The resulting mixed Type 2/Type 3 interference patterns can stem from two independent and geodynamically distinct events, or can alternatively be formed during a single event, as shown by Forbes et al. (2004). The mixed Type 2/Type 3 interference pattern changes to a pure Type 3 pattern towards the west, whereas the eastern continuation of the OSC is unknown due to the tectonic boundary of the Brenner fault. Nevertheless future work should focus on the comparison of the OSC to the Bundschuh complex east of the Tauern window, a unit which is not unequivocally correlated with the OSC (Schmid et al., 2004; Neubauer et al., 2007).

7. Conclusion

Detailed structural mapping allows the determination of a relative chronology of deformation phases and the recognition of fold interferences in the OSC. Yet on a more regional scale, these small scale observations might not hold true because of lithological controls on folding (rock type, thickness variations, etc.), mainly non-cylindrical folds and variable amplitudes depending on their location in the polyphase deformed geometry. Our combination of local mapping and incorporation in a regional geological map, revealed a mixed Type 2/Type 3 interference pattern for the pre-Alpine two-stage folding. The unequivocal pre-Mesozoic character of the first two phases of deformation becomes clear when comparing their structural elements to those of the unconformably overlying Permomesozoic cover in this area. Four known younger deformation phases (ductile and brittle) affected both the basement (OSC) and its cover (BM) and range from Cretaceous to sub-recent.

Reducing the number of originally mapped lithologies by summarizing them to reasonable entities clarifies the structural framework of the OSC and reveals the main outcrop pattern of the region. Although we are aware of possible oversimplifications, we are confident that the main lithological ele-

© Österreichische
Geologische Gesellschaft/Austria; download unter www.geol-ges.at/ und www.biologiezentrum.at

ments, structural evolution and, eventually, the structural geometry can be inferred by this approach.

Acknowledgements

We would like to thank Djordje Grujić, Franz Neubauer and Michael Wagreich for their constructive and detailed reviews. Furthermore, we thank Rainer Brandner for his contribution to questions about the Brenner Mesozoic, Hannah Pomella for her help with GIS-software, and Benoit Saumur for editing an early version of this manuscript.

References

Alsop, G.I. and Carreras, J., 2007. The structural evolution of sheath folds: A case study from Cap de Creus, Journal of Structural Geology, 29, 1915-1930.

Bernhard, F., Klötzli, U.S., Thöni, M. and Hoinkes, G., 1996. Age, origin and geodynamic significance of a polymetamorphic felsic intrusion in the Ötztal Crystalline Basement, Tirol, Austria. Mineralogy and Petrology, 58, 171-196.

Brandner, R., Resch, W. and Reiter, F., 2003. Das Brennermesozoikum. Sedimentäre Faziesentwicklungen in metamorphen Gesteinen und tektonische Konsequenzen. In: M. Rockenschaub (ed.), Arbeitstagung der Geologischen Bundesanstalt. Geologische Bundesanstalt, Trins, pp. 95-98.

Brandner, R. and Reiter, F., 2004. Geologische Karte der Kalkkoegel, 1:25,000. Bund-/Bundesländerprojekt TC 12 (unpublished).

Dietrich, H., 1983. Zur Petrologie und Metamorphose des Brennermesozoikums (Stubaier Alpen, Tirol). Tschermak's Mineralogische und Petrographische Mitteilungen, 3, 235-257.

Flöss, D., 2009. Tektonometamorphe Entwicklung der westlichen Austroalpinen Einheiten: Geometrie und Kinematik der eoalpinen Kollision (Texel Komplex, Südtirol). PhD Thesis, University of Innsbruck, Innsbruck, 135 pp.

Forbes, C.J., Betts, P.G., Lister, G.S., 2004. Synchronous development of Type 2 and Type 3 fold interference patterns: evidence for recumbent sheath folds in the Allendale Area, Broken Hill, NSW, Australia. Journal of Structural Geology, 26, 113-126.

Förster, H., 1967. Kristallisation und Tektonik des Schneeberger Geteinszuges. Geologische Rundschau, 56, 480-494.

Förster, H. and Schmitz-Wiechowski, A., 1970. Zur Tektonik im Bereich der Brennerlinie. Geologische Rundschau, 59, 2, 637-648.

Frank, W., Kralik, M., Scharbert, S. and Thöni, M., 1987. Geochronological data from the Eastern Alps. In: H.W. Flügel and P. Faupl (eds.), Geodynamics of the Eastern Alps. Deuticke Vienna, pp. 272-281.

Frisch, W., Kuhlemann, J., Dunkl, I. and Brügel, A., 1998. Palinspastic reconstruction and topographic evolution of the Eastern Alps during late Tertiary tectonic extrusion. Tectonophysics, 297, 1–15.

Froitzheim, N., Schmid, S. and Conti, P., 1994. Repeated change from crustal shortening to orogenparallel extension in the Austroalpine units of Graubünden. Eclogae geologicae Helvetiae, 87, 559-612.

Fügenschuh, B., 1995. Thermal and kinematic history of the Brenner area (Eastern Alps, Tyrol). PhD Thesis, ETH Zürich, 224 pp.

Fügenschuh, B., Seward, D. and Mancktelow, N.S., 1997. Exhumation in a convergent orogen; the western Tauern window. Terra Nova, 9, 213-217.

Fügenschuh, B., Mancktelow, N.S. and Seward, D., 2000. The Cretaceous to Neogene cooling and exhumation history of the Oetztal-Stubai basement complex, Eastern Alps: a structural and fission-track study. Tectonics, 20, 905-918.

Ghosh, S.K., 1974. Strain distribution in superposed buckling folds and the problem of reorientation of early lineations. Tectonophysics, 21, 249-272.

Ghosh, S.K., Mandal, N., Khan, D. and Deb, S.K., 1992. Modes of superposed buckling in single layers controlled by initial tightness of early folds. Journal of Structural Geology, 14, 4, 381-394.

Grujić, D., 1993. The influence of initial fold geometry on Type 1 and Type 2 interference patterns: an experimental approach. Journal of Structural Geology, 15, 293-307.

Grujić, D. and Mancktelow, N.S., 1995. Folds with axes parallel to the extension direction: an experimental study. Journal of Structural Geology, 17, 279-291.

Hammer, W., 1929. Geologische Spezialkarte der Republik Österreich, Ötzthal (1:75,000). Geologische Bundesanstalt, Wien.

Hoernes , S. and Hoffer, E., 1973. Der Amphibolitzug des mittleren Ötztales (Tirol). Veröffentlichungen des Museums Ferdinandeum, 53, 159-180.

Hoernes, S. and Friedrichsen, H., 1978. Oxygen and Hydrogen Isotope Study of the Polymetamorphic Area of the Northern Ötztal-Stubai Alps (Tyrol), Contributions to Mineralogy and Petrology, 67, 305-315.

Hoinkes, G., Purtscheller, F. and Tessadri, R., 1982. Polymetamorphose im Ostalpin westlich der Tauern (Ötztaler Masse, Schneeberger Zug, Brennermesozoikum) - Zusammenfassung der petrographischen Neuergebnisse. Geologisch-Paläontologische Mitteilungen Innsbruck, 12, 95-113.

© Österreichische
Geologische Gesellschaft/Austria; download unter www.geol-ges.at/ und www.biologiezentrum.at

Hoinkes, G., Kostner, A. and Thöni, M., 1991. Petrologic Constraints for Eoalpine Eclogite Facies Metamorphism in the Austroalpine Ötztal Basement. Mineralogy and Petrology, 43, 237-254.

Hoinkes, G. and Thöni, M., 1993. Evolution of the Ötztal-Stubai, Scarl-Campo and Ulten basement units. – In: J.F. von Raumer and F. Neubauer (eds.), Premesozoic Geology in the Alps. Springer, Heidelberg, pp. 485-494.

Klötzli-Chowanetz, E., Klötzli, U. and Koller, F., 1997. Lower Ordovician migmatisation in the Ötztal crystalline basement (Eastern Alps, Austria): linking U-Pb and Pb-Pb dating with zircon morphology. Schweizerische Mineralogische und Petrographische Mitteilungen, 77, 315-324.

Köhler, M., 1978. Brennerflachbahn, Projekt 1978. Ergebnisse der geologischen Untersuchungen. Geologisch-Paläontologische Mitteilungen Innsbruck, 8, 1-99.

Konzett, J. and Hoinkes, G., 1996. Paragonite-hornblende assemblages and their petrological significance: an example from the Austroalpine Schneeberg Complex, Southern Tyrol, Italy. Journal of Metamorphic Geology, 14, 85-101.

Krois, P., 1989. Untersuchungen an den basalen klastischen Gesteinen des Brennermesozoikums (Stubaier Alpen, Tirol). PhD Thesis, University of Innsbruck, Innsbruck, 116 pp.

Krois, P., Stingl, V. and Purtscheller, F., 1990. Metamorphosed weathering horizon from the Oetztal-Stubai crystalline complex (Eastern Alps, Austria). Geology, 18, 1095-1098.

Langheinrich, G., 1965. Zur Tektonik und Metamorphose des zentralalpinen Permomesozoikums westlich der Brennersenke. Nachrichten der Akademie der Wissenschaften zu Göttingen - II. mathematisch-physikalische Klasse, 10, 133-149.

Maggetti, M. and Flisch, M., 1993. Evolution of the Silvretta Nappe. In: J. von Raumer and F. Neubauer (eds.): Pre-Mesozoic Geology in the Alps. Springer, Berlin-Heidelberg, pp. 469-484.

Miller, C., 1970. Petrology of some eclogites and metagabbros of the Oetztal Alps, Tirol, Austria. Contributions to Mineralogy and Petrology, 28, 42-56.

Miller, C. and Thöni, M., 1995. Origin of eclogites from the Austroalpine Ötztal basement (Tirol, Austria): geochemistry and Sm-Nd vs. Rb-Sr isotope systematic. Chemical Geology (Isotope Geoscience Section), 122, 199-225.

Neubauer, F., Hoinkes, G., Sassi, F.P., Handler, R., Höck, V., Koller, F. and Frank, W., 1999. Pre-Alpine metamorphism of the Eastern Alps. Schweizerische Mineralogische und Petrographische Mitteilungen, 79, 41-62.

Neubauer, F., Friedl, G., Genser, J., Handler, R., Mader, D. and Schneider, D., 2007. Origin and tectonic evolution of the Eastern Alps deduced from dating of detrital white mica: a review. Austrian Journal of Earth Sciences, 100, 8-23.

Odonne, F. and Vialon, P., 1987. Hinge migration as a mechanism of superimposed folding. Journal of Structural Geology, 9, 835-844.

Ortner, H., Reiter, F. and Brandner, R. 2006. Kinematics of the Inntal shear zone – sub-Tauern ramp fault system and the interpretation of the TRANSALP seismic section, Eastern Alps, Austria. Tectonophysics, 414, 241-258.

Pomella, H., Flöss, D., Speckbacher, R. and Fügenschuh, B., 2010. The evolution of the Austroalpine nappe stack in the hanging wall of the Giudicarie fault system. Journal of Alpine Geology – Pangeo Austria 2010, 52, 202.

Purtscheller, F., 1969. Petrographische Untersuchungen an Alumosilikatgneisen des Ötztaler-Stubaier Altkristallins. Tschermaks Mineralogische und Petrographische Mitteilungen, 13, 35-54.

Purtscheller, F., 1971. Ötztaler und Stubaier Alpen. Sammlung Geologischer Führer, 53. Borntraeger, Berlin-Stuttgart, 111 pp.

Purtscheller, F., 1978. Ötztaler und Stubaier Alpen. Sammlung Geologischer Führer, 53, 2. Auflage, Borntraeger, Berlin-Stuttgart, 128 pp.

Ramsay, J.G., 1967. Folding and Fracturing of Rocks. McGraw-Hill, New York, 568 pp.

Ramsay, J.G. and Huber, M.I., 1987. The techniques of Modern Structural Geology, Vol. 2, Folds and Fracture. Academic Press, London, 391 pp.

Reiter, F., Lenhardt, W.A., Brandner, R., 2005. Indications for activity of the Brenner Normal Fault zone (Tyrol, Austria) from seismological and GPS data. Austrian Journal of Earth Sciences, 97, 16-23.

Rockenschaub, M., Brandner, R., Decker, K., Priewalder, H. and Reiter, F. 2003. Geologie und Tektonik westlich des Wipptals. In: M. Rockenschaub (ed.), Arbeitstagung der Geologischen Bundesanstalt. Geologische Bundesanstalt, Trins, pp. 79-94.

Royden, L., Horváth, F., Burchfiel, B.C. 1982. Transform faulting, extension and subduction in the Carpathian Pannonian region. Geological Society of America Bulletin, 73, 717-725.

Schmid, S.M. and Haas, R., 1989. Transition from near-surface thrusting to intrabasement decollement, Schlinig thrust, Eastern Alps. Tectonics, 8, 697-718.

Schmid, S.M. and Froitzheim, N., 1993. Olique slip and block rotation along the Engadine line. Eclogae geologicae Helvetiae, 86, 569-593.

© Österreichische
Geologische Gesellschaft/Austria; download unter www.geol-ges.at/ und www.biologiezentrum.at

Schmid, S.M., Fügenschuh, B., Kissling, E. and Schuster, R., 2004. Tectonic map and overall architecture of the Alpine orogen. Eclogae geologicae Helvetiae, 97, 93-117.

Schmidegg, O., 1956. Neues zur Geologie des Brennermesozoikums (Blaserdecke und Serleskamm). Mitteilungen der Österreichischen Geologischen Gesellschaft, 48, 271-295.

Schmidegg, O., 1964. Die Ötztaler Schubmasse und ihre Umgebung. Verhandlungen der Geologischen Bundesanstalt, 1964, 27-46.

Schuster, R. and Frank, W., 1999. Metamorphic evolution of the Austroalpine units east of the Tauern window: indications for Jurassic strike slip tectonics. Mitteilungen der Gesellschaft der Geologie- und Bergbaustudenten in Österreich, 42, 37-58.

Schuster, R., Koller, F., Hoeck, V., Hoinkes, G. and Bousquet, R., 2004. Explanatory notes to the map: metamorphic structure of the Alps – metamorphic evolution of the Eastern Alps. Mitteilungen der Österreichischen Mineralogischen Gesellschaft, 149, 63-87.

Schweigl, J., 1995. Neue geochronologische und isotopengeologische Daten zur voralpidischen Entwicklungsgeschichte im Ötztalkristallin (Ostalpen). Jahrbuch der Geologischen Bundesanstalt, 138, 131-149.

Simón, J.L., 2004. Superposed buckle folding in the eastern Iberian Chain, Spain. Journal of Structural Geology, 26, 1447-1464.

Skjernaa, L., 1975. Experiments on superimposed buckle folding. Tectonophysics, 27, 255-270.

Söllner, F. and Hansen, B.T., 1987. "Pan-afrikanisches" und "kaledonisches" Ereignis im Ötztal-Kristallin der Ostalpen: Rb-Sr- und U-Pb-Altersbestimmungen an Migmatiten und Metamorphiten. Jahrbuch der Geologischen Bundesanstalt, 130, 529-569.

Sölva, H., Grasemann, B., Thöni, M., Thiede, R. and Habler, G., 2005. The Schneeberg Fault Zone: Normal faulting associated with Cretaceous SE-directed extrusion in the Eastern Alps (Italy/Austria). Tectonophysics, 401, 143-166.

Speckbacher, R., 2009. Die tektonometamorphe Entwicklung des Texel Komplexes: Strukturgeologie im Pfossental, Südtirol. PhD Thesis, University of Innsbruck, Innsbruck, 129 pp.

Tessadri, R., 1981. Metamorphose am Ostende des Schneeberger Zuges (Sterzing, Südtirol). PhD Thesis, University of Innsbruck, Innsbruck, 95 pp.

Thöni, M., 1980. Zur Westbewegung der Ötztaler Masse, Räumliche und zeitliche Fragen an der Schlinigüberschiebung. Mitteilungen der Gesellschaft der Geologie- und Bergbaustudenten in Österreich, 26, 247-275.

Thöni, M., 1981. Degree and evolution of the Alpine metamorphism in the Austroalpine unit W of the Hohe Tauern in the light of K/Ar and Rb/S rage determinations on micas. Jahrbuch der Geologischen Bundesanstalt, 124, 111-74.

Thöni, M., 1999. A review of geochronological data from the Eastern Alps. Schweizerische Mineralogische und Petrographische Mitteilungen, 79/1, 209-230.

Thöny, W.F., Tropper, P., Schennach, F., Krenn, E., Finger, F., Kaindl, R., Bernhard, F. and Hoinkes, G., 2008. The metamorphic evolution of migmatites from the Ötztal Complex (Tyrol, Austria) and constraints on the timing of the pre-Variscan high-T event in the Eastern Alps. Swiss Journal of Geosciences, 101, 111-126.

Tollmann, A., 1963. Ostalpen-Synthese. Deuticke, Wien, 256 pp.

Tollmann, A., 1977. Geologie von Österreich, Bd. 1, Die Zentralalpen. Deuticke, Wien, 766 pp.

Tropper, P. and Recheis, A., 2003. Garnet zoning as a window into the metamorphic evolution of a crystalline complex: the northern and central Austroalpine Ötztal-Complex as a polymorphic example. Mitteilungen der Österreichischen Geologischen Gesellschaft, 94 (2001), 27-53.

Van Gool, J., Kemme, M. and Schreurs, G., 1987. Structural investigations along a E-W cross-section in the Southern Ötztal Alps. In: H.W. Flügel and P. Faupl (Eds.), Geodynamics of the Eastern Alps. Deuticke, Wien, pp. 215-225.

Veltman, C., 1986. Zur Polymetamorphose pelitischer Gesteine im Ötztal-Stubaier Altkristallin. PhD Thesis, University of Innsbruck, Innsbruck, 164 pp.

Von Raumer, J. and Neubauer, F., 1993. Correlation and evolution of the Alpine basement. In: J. von Raumer and F. Neubauer (eds.), Pre-Mesozoic Geology in the Alps. Springer, Berlin, pp. 625–639.

Received: 23 October 2012
Accepted: 6 November 2013

Mathias EGGLSEDER[1)2)*)], Bernhard FÜGENSCHUH[1)]

[1)] Department of Geology and Paleontology, University of Innsbruck, Austria;

[2)] School of Geosciences, Monash University, Melbourne, Australia;

[*)] Corresponding author, mathias.egglseder@monash.edu

ZOBODAT - www.zobodat.at

Zoologisch-Botanische Datenbank/Zoological-Botanical Database

Digitale Literatur/Digital Literature

Zeitschrift/Journal: Austrian Journal of Earth Sciences

Jahr/Year: 2013

Band/Volume: 106_2

Autor(en)/Author(s): Egglseder Mathias, Fügenschuh Bernhard

Artikel/Article: Pre-Alpine fold interference patterns in the northeastern Oetztal-Stubai-Complex (Tyrol, Austria). 63-74